CAMBRIDGE
UNIVERSITY PRESS

Article

Cuatrocapaite-(NH₄) and cuatrocapaite-(K), two new minerals from the Torrecillas mine, Iquique Province, Chile, related to lucabindiite and gajardoite

Anthony R. Kampf[1]* [iD] , Nikita V. Chukanov[2], Gerhard Möhn[3], Maurizio Dini[4], Arturo A. Molina Donoso[5] and Henrik Friis[6]

[1]Mineral Sciences Department, Natural History Museum of Los Angeles County, 900 Exposition Boulevard, Los Angeles, CA 90007, USA; [2]Institute of Problems of Chemical Physics, Russian Academy of Sciences, Chernogolovka, Moscow region, 142432 Russia; [3]Dr.-J.-Wittemannstrasse 5, 65527 Niedernhausen, Germany; [4]Pasaje San Agustin 4045, La Serena, Chile; [5]Los Algarrobos 2986, Iquique, Chile; and [6]Natural History Museum, University of Oslo, Postboks 1172, Blindern, 0318, Oslo, Norway

Abstract

The new minerals cuatrocapaite-(NH₄) (IMA2018-083) and cuatrocapaite-(K) (IMA2018-084) are the NH₄- and K-dominant members of a series with the general formula $(NH_4,K)_3(NaMg\square)(As_2O_3)_6Cl_6\cdot16H_2O$. Both minerals were found at the Torrecillas mine, Iquique Province, Chile, where they occur as secondary alteration phases. Both minerals occur as hexagonal tablets up to ~0.3 mm in diameter. They are transparent, with a vitreous lustre and white streak. For both, the Mohs hardness is *ca.* 2½, the crystals are somewhat flexible, but not elastic, the fracture is irregular and the cleavage is perfect on {001}. The measured densities are 2.65(2) and 2.76(2) g/cm³ for the NH₄- and K-dominant species, respectively. Optically, cuatrocapaite-(NH₄) is uniaxial (–) with ω = 1.779(3) and ε = 1.541(3) and cuatrocapaite-(K) is uniaxial (–) with ω = 1.777(3) and ε = 1.539(3) (white light). The minerals are insoluble in acids, but decompose in NaOH(aq). The empirical formulas, determined from electron-microprobe analyses, are $(NH_4)_{2.48}Na_{1.66}Mg_{0.87}K_{0.09}(As_{12}O_{18.05})Cl_{5.88}\cdot16.02H_2O$ and $K_{2.68}Na_{1.33}Mg_{0.93}(NH_4)_{0.31}(As_{12}O_{18.01})Cl_{6.16}\cdot16.04H_2O$. The minerals are trigonal, space group $R\bar{3}m$; the cuatrocapaite-(NH₄) cell parameters are *a* = 5.25321(19), *c* = 46.6882(19) Å, *V* = 1115.80(9) Å³ and *Z* = 1; the cuatrocapaite-(K) cell parameters are *a* = 5.2637(15), *c* = 46.228(8) Å, *V* = 1109.2(7) Å³ and *Z* = 1. The structures, refined for cuatrocapaite-(NH₄) to R_1 = 1.78% for 544 $I_o > 2\sigma I$ reflections, contain four types of layers: (1) a planar neutral As₂O₃ (arsenite) sheet; (2) an (NH_4^+,K^+) layer that links adjacent arsenite sheets; (3) a Cl⁻ layer placed on the As side of each arsenite; and (4) a layer containing partially occupied Na, Mg and H₂O sites that is flanked on either side by Cl layers. The layer sequence for the type 1, 2 and 3 layers is identical to the Cl–As₂O₃–K–As₂O₃–Cl layer sequence in the structures of lucabindiite and gajardoite.

Introduction

The small, long-inactive Torrecillas mine in the northern Atacama Desert of Chile was probably discovered and first worked during the guano mining boom of the early 19th century (Mortimer, *et al.*, 1971). The once-important Pabellón de Pica guano deposit is only ~7 km north of Torrecillas Hill. Although the veins that were exploited at Torrecillas are particularly rich in arsenic, the early miners were most likely to be working the veins for copper and, perhaps, were hoping to find gold. The deposit apparently was worked later for arsenic, as reported by Pimentel (1978), who also noted that the mine was probably finally abandoned several years prior to 1950. Based upon the very limited extent of the workings, the mine clearly was never a significant producer.

In recent years, our investigations on the minerals of this unusual deposit have yielded many new mineral species. Including the two new minerals reported herein, cuatrocapaite-(NH₄) and cuatrocapaite-(K), eighteen new minerals have now been described from this deposit. All of these, except leverettite, CoCu₃Cl₂(OH)₆ (Kampf *et al.*, 2013), contain essential arsenic. Twelve are arsenates and five are arsenites [see Kampf *et al.* (2019) for a complete listing]; cuatrocapaite-(NH₄) and cuatrocapaite-(K) are arsenites.
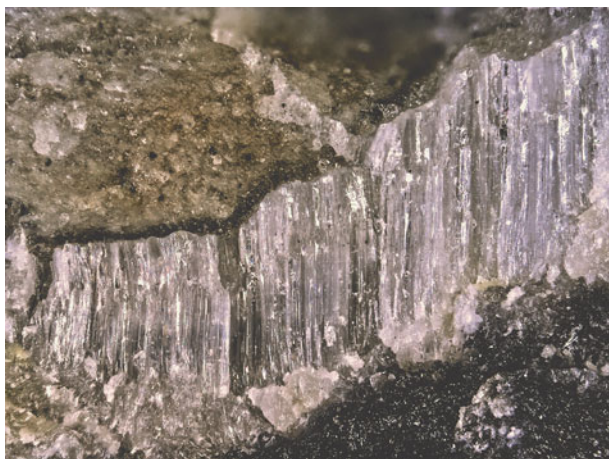
The name 'cuatrocapaite' is in allusion to the structure, which consists of four (*cuatro* in Spanish) different types of layers (*capa* in Spanish): (1) [As₂O₃]; (2) [(NH₄),K]; (3) [Cl₆]; and (4) [(Na, Mg,)₃(H₂O)₁₆]. The -(NH₄) and -(K) suffixes indicate the dominant cations in the large-cation layer (2). The IPA pronunciation of cuatrocapaite is (/kwɑː troʊ ˈkɑː pɑː aɪt/). The new minerals and their names, cuatrocapaite-(NH₄) (IMA2018-083, Kampf *et al.*, 2018*a*) and cuatrocapaite-(K) (IMA2018-084, Kampf *et al.*, 2018*b*), have been approved by the Commission on New Minerals, Nomenclature and Classification of the International Mineralogical Association. The description of cuatrocapaite-(NH₄)

Fig. 1. Cuatrocapaite-(NH₄) tablets, some in vermiform stacks, with acicular torrecillasite; field of view 0.6 mm across. Specimen no. 66986.
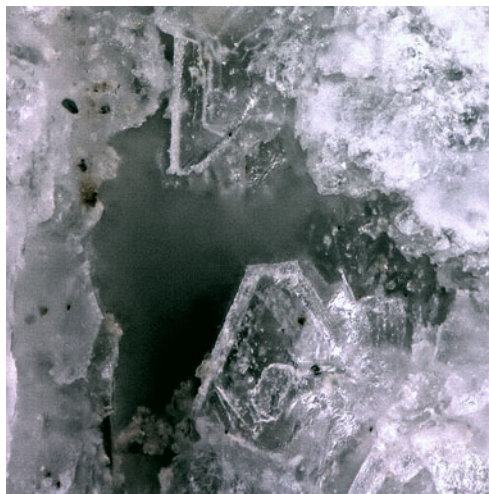

Fig. 3. Cuatrocapaite-(K) tablets; field of view 0.4 mm across. Specimen no. 66987.

Fig. 2. Cuatrocapaite-(NH₄) satin-spar-like vein filling; field of view 1.7 mm across. Specimen no. 66984.

Fig. 4. Tablets of the I-rich NH₄-analogue of lucabindiite exhibiting apparent twinning by rotation on [001]; field of view 0.63 mm across. Specimen no. 66985.

is based upon four cotype specimens. Three are deposited in the collections of the Natural History Museum of Los Angeles County, 900 Exposition Boulevard, Los Angeles, CA 90007, USA with catalogue numbers 66984, 66985 and 66986. One is deposited in the collection of the Fersman Mineralogical Museum of the Russian Academy of Sciences, Moscow, Russia with registration number 5255/1. The description of cuatrocapaite-(K) is based upon one holotype specimen deposited in the collections of the Natural History Museum of Los Angeles County, catalogue number 66987.

Occurrence

The Torrecillas mine is located on Torrecillas Hill, Iquique Province, Tarapacá Region, Chile (~20°58′13″S, 70°8′17″W). Four different rock units are exposed on the hill. The Coastal Range Batholith (mainly gabbros) extends from the seashore to the Pan-American Road along the base of Torrecillas Hill. At the foot of Torrecillas Hill is a small area of contact metamorphic rocks in which garnet crystals occur in metamorphosed shales. Higher on the hill, the rocks are predominantly porphyritic andesitic lavas of

the Jurassic La Negra Formation (*cf*. Oliveros *et al*., 2007). The Torrecillas deposit, in which the new minerals are found, consists of two main veins rich in secondary arsenic and copper minerals that intersect metamorphosed marine shales and lavas. These mineralised veins are genetically related to the aforementioned porphyritic andesitic lavas. More information on the geology and mineralogy of the area is provided by Gutiérrez (1975).

The rare secondary chlorides, arsenates and arsenites have been found at three main sites on the hill: an upper pit measuring ~8 m long and 3 m deep, a lower pit ~100 m from the upper pit and measuring ~5 m long and 3 m deep, and a mine shaft adjacent to the lower pit and lower on the hill. Cuatrocapaite-(NH₄) was found in November of 2015 in a recent excavation a few metres above the shaft by one of the authors (AAMD). Cuatrocapaite-(K) was found in January of 2016 near the upper pit by another of the authors (GM), who also collected additional cuatrocapaite-(NH₄) specimens.
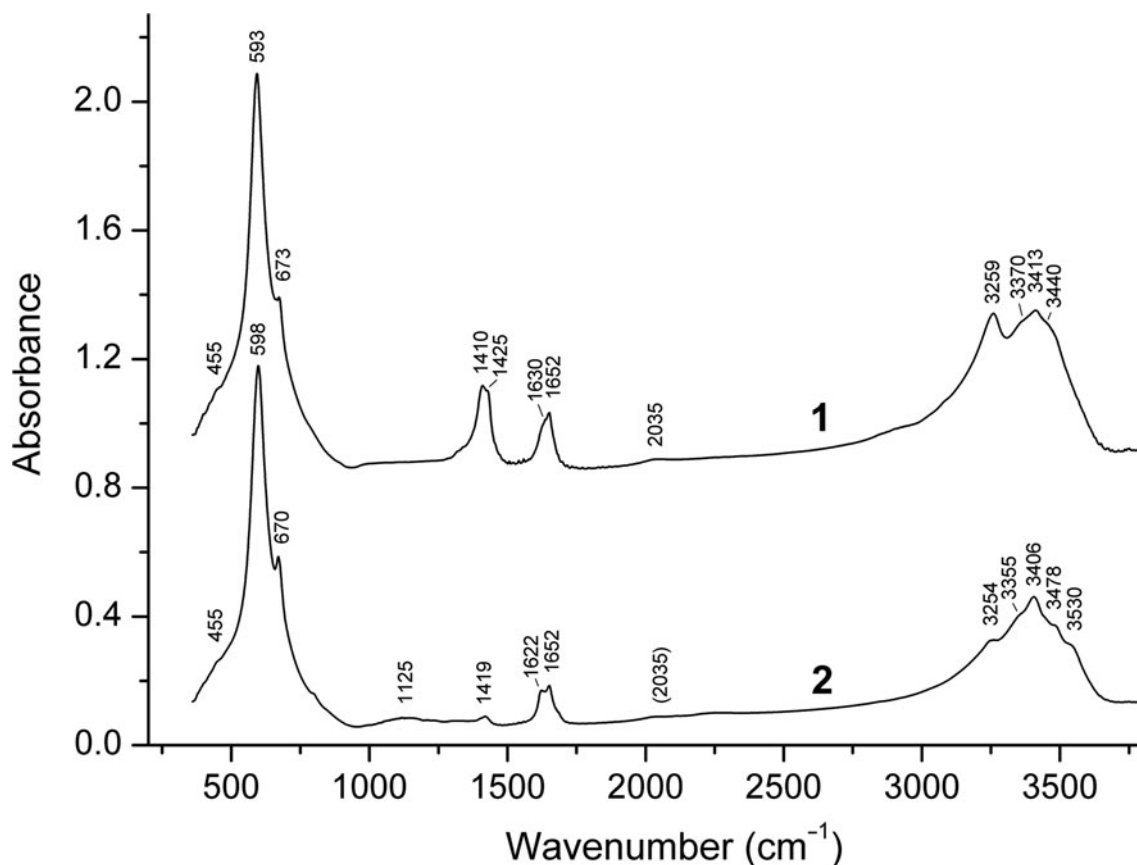
Fig. 5. Powder IR absorption spectra of (1) cuatrocapaite-(NH$_4$) and (2) cuatrocapaite-(K).

Both new minerals are low-temperature secondary alteration phases occurring on matrix consisting of native arsenic, arsenolite and pyrite. Cuatrocapaite-(NH$_4$) is also associated with lavendulan, magnesiokoritnigite, torrecillasite and the I-rich NH$_4$-analogue of lucabindiite (currently under study). Cuatrocapaite-(K) is also associated with anhydrite, gypsum, lavendulan and torrecillasite. The secondary As-rich assemblages at the Torrecillas deposit are interpreted as having formed under hyperarid conditions from the oxidation of native arsenic, and possibly other As-bearing primary phases, coupled with reaction with underground brines rich in mobile cations such as K$^+$, Na$^+$, NH$_4^+$, Ca^{2+} and Mg^{2+} (*cf.* Cameron *et al.*, 2007). Following the exhumation of Torrecillas Hill, it is possible that long-term exposure to the frequent dense coastal fogs (*cf.* Rech *et al.*, 2003; Wang *et al.*, 2014; Kampf *et al.*, 2019) caused continued near-surface alteration coupled with very late-stage secondary mineral formation.

Physical and optical properties

Both cuatrocapaite-(NH$_4$) and cuatrocapaite-(K) occur as hexagonal plates, flattened on {001} and bounded by {100}, up to ~300 μm in diameter. The pyramidal forms {10ℓ} and {01ℓ} are present on some crystals, with measurements on cuatrocapaite-(NH$_4$) plates indicating ℓ values in the 12 to 18 range. Cuatrocapaite-(NH$_4$) plates sometimes grow in vermiform stacks (Fig. 1) and in satin-spar-like vein fillings (Fig. 2) and the mineral is also found as white powdery coatings. Most cuatrocapaite-(K) crystals have been observed in massive intergrowths, but freestanding crystals in vugs do occur (Fig. 3).

No twinning was observed for either mineral. Crystals of the I-rich, NH$_4$-analogue of lucabindiite occurring in association with cuatrocapaite-(NH$_4$), are very similar in appearance, but exhibit apparent twinning by rotation on [001] (Fig. 4).

Crystals are colourless and transparent, with a white streak. Crystals have a vitreous to pearly lustre, while vein fillings of cuatrocapaite-(NH$_4$) have a silky lustre. The minerals do not fluoresce in long- or short-wave ultraviolet light. The Mohs hardness for both is 2½, based on scratch tests, and thin plates are flexible, but not elastic. Cleavage is perfect on {001}. The densities for cuatrocapaite-(NH$_4$) and cuatrocapaite-(K), measured by flotation in methylene iodide – toluene are 2.65(2) and 2.76(2) g/cm^3, respectively, and their calculated densities, based on the empirical formulas, are 2.667 and 2.771 g/cm^3, respectively.

At room temperature, the minerals are not readily soluble in water or acids (including concentrated HCl, H$_2$SO$_4$ and HNO$_3$). They decompose rapidly in aqueous solution of NaOH forming a nearly transparent residue of Mg(OH)$_2$. As an added confirmation for the presence of NH$_4^+$ in cuatrocapaite-(NH$_4$), a microchemical test was performed. The mineral was heated in a melting-point tube, yielding sublimates (from hot to cold) presumed to be (1) As$_2$O$_3$ (as arsenolite octahedra), (2) NH$_4$Cl and (3) H$_2$O. When placed in Na$_3$[Co(NO$_2$)$_6$] solution, the presumed NH$_4$Cl sublimate yielded an orange precipitate of (NH$_4$)$_2$Na[Co(NO$_2$)$_6$], thereby confirming the presence of NH$_4^+$.

Optically, both minerals are uniaxial (–) and nonpleochroic. The indices of refraction for cuatrocapaite-(NH$_4$) are ω = 1.779(3) and ε = 1.541(3) and those for cuatrocapaite-(K) are ω = 1.777(3) and ε = 1.539(3) (measured in white light). The Gladstone–Dale

Table 1. Analytical data (wt.%) for cuatrocapaite-(NH$_4$) and cuatrocapaite-(K).

Constituent	Cuatrocapaite-(NH$_4$)			Cuatrocapaite-(K)			Probe standard
	Mean	Range	S.D.	Mean	Range	S.D.	
(NH$_4$)$_2$*	3.61 ± 0.2			0.44 ± 0.1			
Na$_2$O	2.85	2.58–3.03	0.20	2.26	2.13–2.44	0.14	Albite
K$_2$O	0.23	0.19–0.31	0.06	6.94	6.44–7.41	0.39	Sanidine
MgO	1.94	1.82–2.14	0.14	2.06	1.56–2.54	0.40	Diopside
As$_2$O$_3$	65.79	65.02–66.63	0.58	65.39	64.73–66.06	0.55	As
Cl	11.55	11.06–12.06	0.41	12.04	11.63–12.38	0.31	NaCl
H$_2$O§	16.11			15.56			
–O = Cl	−2.61			−2.72			
Total	99.47			101.97			

*Measured by gas chromatography for cuatrocapaite-(NH$_4$); estimated by IR spectroscopy for cuatrocapaite-(K)
§Calculated based on the ideal formula
S.D. – Standard deviation

Table 2. Powder X-ray data (*d* in Å) for cuatrocapaite-(NH$_4$).

I_{obs}	I_{calc}	d_{obs}	d_{calc}	*hkl*
100	**100**	**15.68**	**15.5627**	**0 0 3**
29	28	7.80	7.7814	0 0 6
56	**56**	**5.20**	**5.1876**	**0 0 9**
35	13, 9	4.518	4.5280, 4.4654	1 0 1, 0 1 2
3	2	4.212	4.2388	1 0 4
14	6, 4	3.848	3.8907, 3.7584	0 0 12, 1 0 7
15	11	3.594	3.5880	0 1 8
42	**28**	**3.256**	**3.2583**	**1 0 10**
32	3, 26	3.111	3.1125, 3.1035	0 0 15, 0 1 11
	3		2.8189	1 0 13
71	**33, 2, 8**	**2.625**	**2.6266, 2.5938, 2.5900**	**1 1 0, 0 0 18, 1 1 3**
41	**23, 5**	**2.490**	**2.4887, 2.4562**	**1 1 6, 1 0 16**
47	**6, 28**	**2.349**	**2.3512, 2.3433**	**0 1 17, 1 1 9**
	2		2.2232	0 0 21
14	3, 2, 3	2.145	2.1621, 2.1529, 2.1194	1 0 19, 0 2 7, 2 0 8
	1		2.0769	0 1 20
	2		2.0449	0 2 10
15	8, 1	2.0105	2.0074, 2.0049	1 1 15, 2 0 11
	1		1.9232	1 0 22
	1		1.8792	2 0 14
	1		1.8538	0 1 23
26	17	1.8486	1.8456	1 1 18
4	5	1.7949	1.7940	0 2 16
7	5	1.7615	1.7518	2 0 17
12	2, 1, 2, 2	1.7215	1.7292, 1.7276, 1.7184, 1.7149	0 0 27, 1 0 25, 2 1 1, 1 2 2
	1		1.6970	1 1 21
12	1, 2, 1, 3	1.6602	1.6703, 1.6693, 1.6651, 1.6494	0 1 26, 0 2 19, 2 1 7, 1 2 8
	1		1.6292	2 0 20
10	6	1.6123	1.6136	2 1 10
2	4	1.5949	1.5937	1 2 11
5	3, 1, 1	1.5636	1.5633, 1.5517, 1.5509	1 1 24, 0 2 22, 2 1 13
16	7, 2, 1	1.5171	1.5165, 1.5145, 1.5093	3 0 0, 2 0 23, 0 3 3
8	4, 2	1.4887	1.4885, 1.4814	0 3 6, 2 1 16
31	3, 7, 10, 2	1.4523	1.4574, 1.4556, 1.4443, 1.4434	1 2 17, 3 0 9, 1 1 27, 0 2 25
3	1, 2, 1	1.4111	1.4148, 1.4095, 1.4088	0 0 33, 2 0 26, 2 1 19
3	3	1.3617	1.3633	3 0 15
	1		1.3448	0 2 28
22	6, 1, 4, 2	1.3116	1.3133, 1.3121, 1.3091, 1.3087	2 2 0, 1 2 23, 0 3 18, 2 2 3

The strongest lines are given in bold

compatibilities 1 – (K_p/K_c) for the empirical formulas are both 0.019, in the range of superior compatibility (Mandarino, 2007).

Infrared spectroscopy

In order to obtain infrared (IR) absorption spectra, powdered samples were mixed with anhydrous KBr, pelletised, and analysed using an ALPHA FTIR spectrometer (Bruker Optics) at a resolution of 4 cm^{-1}. Sixteen scans were collected for each mineral. The IR spectrum of an analogous pellet of pure KBr was used as a reference.

Absorption bands in the IR spectrum of cuatrocapaite-(NH$_4$) (curve 1 in Fig. 5) and their assignments are (cm^{-1}; s – strong band, w – weak band, sh – shoulder): 3440sh, 3413s, 3370sh

Table 3. Powder X-ray data (*d* in Å) for cuatrocapaite-(K).

I_{obs}	I_{calc}	d_{obs}	d_{calc}	*hkl*
100	**100**	**15.50**	**15.4093**	**0 0 3**
10	9	7.71	7.7047	0 0 6
32	**24**	**5.13**	**5.1364**	**0 0 9**
18	4, 3	4.50	4.5365, 4.4724	1 0 1, 0 1 2
	1		4.2405	1 0 4
5	3	3.828	3.8523	0 0 12
6	3	3.696	3.7515	1 0 7
12	7	3.580	3.5789	0 1 8
33	**17**	**3.228**	**3.2458**	**1 0 10**
33	**16, 1**	**3.098**	**3.0898, 3.0819**	**0 1 11, 0 0 15**
2	3	2.815	2.8038	1 0 13
69	**18, 7**	**2.621**	**2.6319, 2.5943**	**1 1 0, 1 1 3**
	1		2.5682	0 0 18
25	9	2.489	2.4906	1 1 6
	1		2.4404	1 0 16
36	**12, 2**	**2.339**	**2.3423, 2.3353**	**1 1 9, 0 1 17**
	1		2.2013	0 0 21
	1		2.1545	0 2 7
6	1, 2	2.132	2.1464, 2.1203	1 0 19, 2 0 8
	1		2.0443	0 2 10
11	1, 4	2.0003	2.0036, 2.0014	2 0 11, 1 1 15
	1		1.8391	0 1 23
21	9	1.8355	1.8381	1 1 18
3	2	1.7794	1.7895	0 2 16
2	2	1.7458	1.7468	2 0 17
4	1, 1, 1	1.7145	1.7218, 1.7135, 1.7121	2 1 1, 1 0 25, 0 0 27
3	2	1.6848	1.6885	1 1 21
7	1, 1, 1, 2	1.6540	1.6671, 1.6634, 1.6565, 1.6511	2 1 7, 0 2 19, 0 1 26, 1 2 8
6	3	1.6122	1.6145	2 1 10
6	2	1.5983	1.5942	1 2 11
	1		1.5505	2 1 13
13	3, 1, 1	1.5153	1.5195, 1.5122, 1.5075	3 0 0, 0 3 3, 2 0 23
2	1	1.4863	1.4908	0 3 6
10	2, 1	1.4538	1.4571, 1.4554	3 0 9, 1 2 17
8	1, 4	1.4327	1.4360, 1.4352	0 2 25, 1 1 27

The strongest lines are given in bold

(O–H stretching vibrations of H_2O molecules), 3259 (N–H stretching vibrations of ammonium cations), 2035w (combination mode), 1652, 1630sh (bending vibrations of H_2O molecules), 1425sh, 1410 (bending vibrations of ammonium cations), 1125w (broad; possibly, overlapping bands of combination modes), 673s, 593s (As^{3+}–O stretching vibrations), 455 (Mg–O stretching vibrations combined with librational vibrations of H_2O molecules). The assignment was made based in accordance with ranges for characteristic bands of NH_4^+ cations, H_2O molecules, Mg–O and As^{3+}–O bonds indicated by Chukanov and Chervonnyi (2016) based on a representative collection of IR spectra of minerals (Chukanov, 2014). In particular, the strongest band of Mg–O stretching vibrations is observed in the range 430–460 cm^{-1}; the strongest band of As^{3+}–O stretching vibrations of isolated AsO_3^{3-} groups are observed in the range 500–610 cm^{-1} and shift towards somewhat higher values as a result of polymerisation of AsO_3 triangles. In particular, the strongest IR bands of As^{3+}–O stretching vibrations are observed at 545 and 610 cm^{-1} for $Pb_5(AsO_3)Cl_7$; 556, 605 and 641 cm^{-1} for leiteite; 628 and 654 cm^{-1} for manganarsite; and 532, 568 and 656 cm^{-1} for stenhuggarite (Chukanov, 2014). It should be noted that characteristic bands of As^{4+}–O stretching vibrations are observed in the range from 750 to 900 cm^{-1}.

Absorption bands in the IR spectrum of cuatrocapaite-(K) (curve 2 in Fig. 5) and their assignments are (cm^{-1}): 3530sh, 3478sh, 3406s, 3355sh (O–H stretching vibrations of H_2O molecules), 3254 (N–H stretching vibrations of ammonium cations), 2035w (combination mode), 1652, 1622 (bending vibrations of

Table 4. Data collection and structure refinement details for cuatrocapaite-(NH_4).

Crystal data	
Structural formula*	$[(NH_4)_{2.65}K_{0.35})]_{\Sigma 3}(Na_{1.72}Mg_{0.79})_{\Sigma 2.51}$ $(As_2O_3)_6Cl_6 \cdot 15.44H_2O$
Crystal size (µm)	100 × 100 × 5
Crystal system, space group	Trigonal, $R\bar{3}m$
Temperature (K)	293(2)
Unit-cell dimensions (Å): *a, c*	5.25321(19), 46.6882(19)
V (Å^3)	1115.80(9)
Z	1
Density (for above formula) (g/cm^3)	2.660
Absorption coefficient (mm^{-1})	9.371
Data collection	
Diffractometer	Rigaku Synergy-S
X-ray radiation	Mo*K*α (λ = 0.71073 Å)
F(000)	850
θ range	2.62 to 33.31°
Index ranges	−4 ≤ *h* ≤ 7, −5 ≤ *k* ≤ 7, −68 ≤ *l* ≤ 55
Reflections collected / unique	3366 / 577;
Reflections with $I_o > 2\sigma I$	544
R_{int}	0.028
Completeness to θ = 33.31°	92.8%
Refinement	
Refinement method	Full-matrix least-squares on F^2
Parameters / restraints	44 / 0
Final *R* indices [$F_o > 4\sigma(F)$]	$R_1 = 0.0178$, $wR_2 = 0.0467$
R indices (all data)	$R_1 = 0.0193$, $wR_2 = 0.0470$
GoF	1.080
Extinction coefficient	0.00084(19)
$\Delta\rho_{max}$, $\Delta\rho_{min}$ (*e*$^-$/A^3)	+1.21 / −0.67

$R_{int} = \Sigma|F_o^2 - F_o^2(mean)|/\Sigma[F_o^2]$. GoF = $S = \{\Sigma[w(F_o^2 - F_c^2)^2]/(n-p)\}^{1/2}$. $R_1 = \Sigma||F_o| - |F_c||/\Sigma|F_o|$. $wR_2 = \{\Sigma[w(F_o^2 - F_c^2)^2]/\Sigma[w(F_o^2)^2]\}^{1/2}$; $w = 1/[\sigma^2(F_o^2) + (aP)^2 + bP]$ where *a* is 0.0305, *b* is 0 and *P* is $[2F_c^2 + \text{Max}(F_o^2, 0)]/3$.
*The structural formula reflects the refined site occupancies; no effort has been made to balance the net charge of this formula, which has a net charge of +0.3.

Table 5. Atom coordinates and displacement parameters (Å²) for cuatrocapaite-(NH₄)*.

	x/a	y/b	z/c	U_{eq}	U^{11}	U^{22}	U^{33}	U^{23}	U^{13}	U^{12}
NH₄	0	0	0	0.0353(14)	0.0346(17)	0.0346(17)	0.037(2)	0	0	0.0173(8)
Na	⅓	⅔	0.49518(16)	0.042(2)	0.042(3)	0.042(3)	0.043(4)	0	0	0.0208(16)
Mg	0	0	½	0.027(2)	0.028(3)	0.028(3)	0.026(4)	0	0	0.0139(15)
As1	⅓	⅔	0.39103(2)	0.01142(11)	0.00819(12)	0.00819(12)	0.01788(17)	0	0	0.00409(6)
As2	0	0	0.39093(2)	0.01163(11)	0.00828(12)	0.00828(12)	0.01833(17)	0	0	0.00414(6)
Cl	⅔	⅓	0.42153(2)	0.0298(2)	0.0257(3)	0.0257(3)	0.0381(5)	0	0	0.01287(14)
O	0.16671(13)	0.3334(3)	0.37046(3)	0.0151(3)	0.0134(4)	0.0069(5)	0.0228(6)	−0.0002(4)	−0.0001(2)	0.0034(3)
OWa	0.758(2)	0.8788(11)	0.4646(2)	0.075(5)	0.040(5)	0.116(9)	0.043(5)	0.0012(19)	0.002(4)	0.020(3)
OWb	0.6116(19)	0.6869(17)	0.47412(13)	0.054(2)	0.072(5)	0.060(5)	0.042(3)	−0.002(3)	0.006(3)	0.041(4)

*Site occupancies: N = 0.884(9)N/0.116(9)K, Na = 0.287(9), Mg = 0.264(10), OWa = 0.303(13), OWb = 0.277(8).

Table 6. Selected bond distances (Å) for cuatrocapaite-(NH₄).

NH₄–O × 12	3.1470(7)	Na–OWb × 6	1.721(9)*	As1–O × 3	1.7946(13)
		Na–OWa × 3	2.400(13)	As1–Cl × 3	3.3505(5)
Mg–OWa × 6	1.985(8)*	Na–OWb × 6	2.475(3)	As2–O × 3	1.7929(13)
Mg–OWb × 12	2.230(7)			As2–Cl × 3	3.3525(5)

*Too short for cation–O bonds.

H₂O molecules), 1419w (bending vibrations of ammonium cations), 1125w (broad; possibly, overlapping bands of combination modes), 670s, 598s (As³⁺–O stretching vibrations), and 455 (Mg–O stretching vibrations combined with librational vibrations of H₂O molecules).

For both minerals, splitting of the band of bending vibrations of H₂O molecules (a non-degenerate mode) indicates the presence of locally non-equivalent water molecules in the structure. The IR spectrum of cuatrocapaite-(NH₄) differs from that of cuatrocapaite-(K) in much higher intensities of the NH₄⁺ bands.

Composition

Chemical analyses (3 points for each mineral) were carried out using an electron microprobe (EDS mode, 20 kV and 600 pA. Attempts to use WDS mode, with higher beam current, were unsuccessful because of the instability of the minerals. For cuatrocapaite-(NH₄), the beam was rasterised on an area 16 μm × 16 μm to minimise sample damage. Also for cuatrocapaite-(NH₄), N was analysed by gas chromatography of products of ignition at 1200°C in oxygen flow, by means of a Vario Micro cube analyser (Elementar GmbH, Germany). For cuatrocapaite-(K), is was possible to estimate the content of NH₄ from the IR spectrum using cuatrocapaite-(NH₄) as a standard because in both minerals NH₄⁺ has identical local environments.

For both minerals, H₂O was calculated from the idealised formula. Contents of other elements with atomic numbers >8 are below detection limits. Analytical data are given in Table 1.

The charge-balanced empirical formulas for cuatrocapaite-(NH₄) and cuatrocapaite-(K) (based on 12 As atoms per formula unit) are $(NH_4)_{2.48}Na_{1.66}Mg_{0.87}K_{0.09}(As_{12}O_{18.05})Cl_{5.88} \cdot 16.02H_2O$ and $K_{2.68}Na_{1.33}Mg_{0.93}(NH_4)_{0.31}(As_{12}O_{18.01})Cl_{6.16} \cdot 16.04H_2O$, respectively. The simplified formula for both minerals is $(NH_4, K)_3(Na,Mg,\square)_3(As_2O_3)_6Cl_6 \cdot 16H_2O$ (with K preceding NH₄ in the formula of the K-dominant phase). The ideal formula for cuatrocapaite-(NH₄) is $(NH_4)_3NaMg\square(As_{12}O_{18})Cl_6 \cdot 16H_2O$, which requires (NH₄)₂O 4.37, Na₂O 1.73, MgO 2.25, As₂O₃ 66.34, Cl 11.89, H₂O 16.11, −O = Cl −2.68, total 100.00 wt.%. The
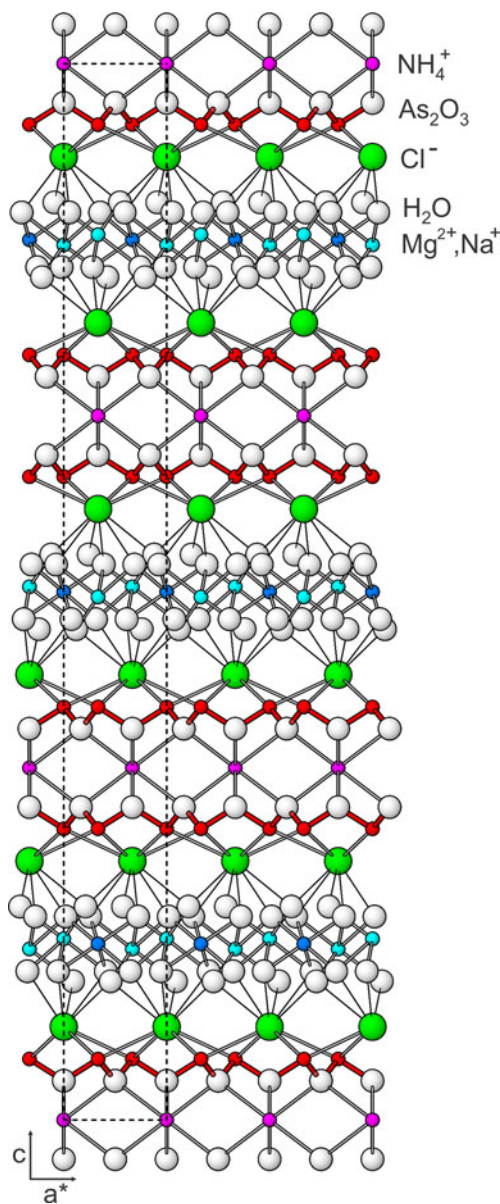
Fig. 6. The structure of cuatrocapaite-(NH₄).

idealised formula for cuatrocapaite-(K) is $K_3NaMg\square(As_{12}O_{18})Cl_6 \cdot 16H_2O$, which requires K₂O 7.63, Na₂O 1.67, MgO 2.18, As₂O₃ 64.07, Cl 11.48, H₂O 15.56, −O = Cl −2.59, total 100.00 wt.%.
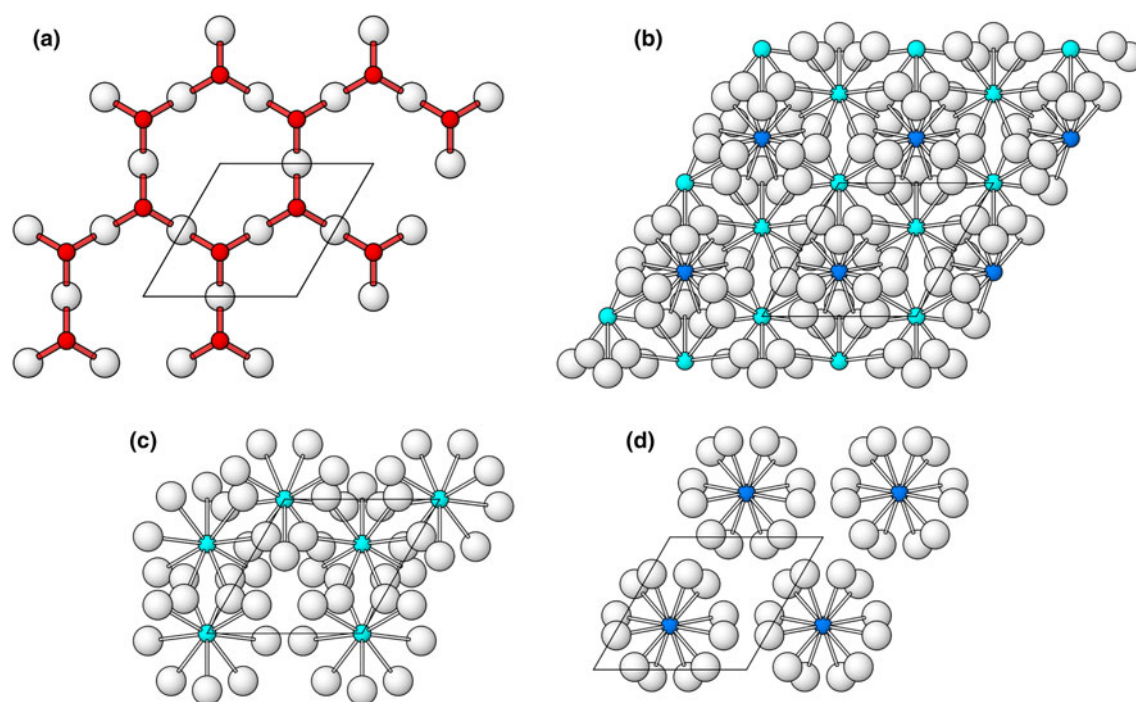
Fig. 7. Selected layer components in the structure of cuatrocapaite-(NH_4) viewed down *c*: (*a*) the As_2O_3 (arsenite) layer, (*b*) the Na–Mg–H_2O layer, (*c*) the Na–H_2O portion of the Na–Mg–H_2O layer, (*d*) the Mg–H_2O portion of the Na–Mg–H_2O layer. The unit-cell outline is shown.

X-ray crystallography and structure refinement

Powder X-ray studies were carried out using a Rigaku R-Axis Rapid II curved imaging plate microdiffractometer, with monochromatic Mo$K\alpha$ radiation. A Gandolfi-like motion on the φ and ω axes was used to randomise the samples and observed *d* values and intensities were derived by profile fitting using *JADE 2010* software (Materials Data, Inc.). The powder data for cuatrocapaite-(NH_4) and cuatrocapaite-(K), presented in Tables 2 and 3, respectively, are quite similar and show good agreement with the patterns calculated from the structure refinements. Unit-cell parameters refined from the powder data using *JADE 2010* with whole pattern fitting are $a = 5.2501(7)$, $c = 46.639(8)$ Å and $V = 1113.3(4)$ Å^3 for cuatrocapaite-(NH_4) and $a = 5.2637(16)$, $c = 46.228(19)$ Å and $V = 1109.2(8)$ Å^3 for cuatrocapaite-(K).

Initial single-crystal X-ray studies were carried out for both cuatrocapaite-(NH_4) and cuatrocapaite-(K) using the same diffractometer and radiation used for the powder studies. Crystals of cuatrocapaite-(K) are generally of poorer quality than those of cuatrocapaite-(NH_4) and our structure data for cuatrocapaite-(K), while confirming it to be isostructural with cuatrocapaite-(NH_4), yielded a much poorer refinement ($R_1 = 6.97\%$ for 263 reflections with $I_o > 2\sigma I$). Rather than report this refinement, herein we provide the details only for the structure refinement for cuatrocapaite-(NH_4). Nevertheless, we confirm that the refinement for cuatrocapaite-(K) is consistent with nearly full occupancy of K at the (K,NH_4) site.

The final cuatrocapaite-(NH_4) structure data were collected on a Rigaku Synergy-S diffractometer equipped with a HyPix-6000HE detector at the Natural History Museum, University of Oslo using monochromatised Mo$K\alpha$ radiation. The Rigaku *CrysAlisPro* software package was used for processing the structure data, including the application of a shape-based absorption correction. An initial structure model was obtained by the charge-flipping method using *SHELXT* (Sheldrick, 2015*a*) in the space group $R\bar{3}m$. Refinement proceeded by full-matrix least-squares on F^2 using *SHELXL-2016* (Sheldrick, 2015*b*). A difference-Fourier map failed to reveal the locations of the H atoms associated with the NH_4^+ cation or with the two partially occupied OW sites. The H sites associated with NH_4^+ are presumed to be disordered, as is commonly the case. The only difference-Fourier peak > 0.42 e^-/A^3 has a magnitude of 1.21 e^-/A^3 (which refines to <5% occupancy by O). This peak at [⅔, ⅓, 0.391], in the centre of the 'cavities' in the As_2O_3 (arsenite) sheet and only 1.42 Å from the Cl site, is assumed to be a refinement artefact. The data collection and refinement details are given in Table 4, atom coordinates and displacement parameters in Table 5 and selected bond distances in Table 6. The crystallographic information file has been deposited with the Principal Editor of *Mineralogical Magazine* and is available as Supplementary material (see below).

Description of the structure

The structure of cuatrocapaite-(NH_4) (Fig. 6) contains four types of layers: (1) a planar neutral As_2O_3 (arsenite) sheet with hexagonal symmetry (Fig. 7*a*); (2) an NH_4^+ layer that links adjacent arsenite sheets *via* bonds to their O atoms; (3) a Cl$^-$ layer placed on the As side of each arsenite sheet with the Cl atoms forming long bonds to the As atoms; and (4) a layer containing partially occupied Na, Mg and H_2O sites (Fig. 7*b,c,d*) that is flanked on either side by Cl layers. The Cl–As_2O_3–NH_4–As_2O_3–Cl layer sequence is identical to the Cl–As_2O_3–K–As_2O_3–Cl layer sequence in the structures of lucabindiite (Garavelli *et al.*, 2013) and gajardoite (Kampf *et al.*, 2016). In lucabindiite, this sequence

repeats itself with no intervening layers, while gajardoite incorporates a disordered Ca–H$_2$O layer and cuatrocapaite-(NH$_4$) incorporates a disordered Na–Mg–H$_2$O layer. Based on the low occupancies of the sites in the Na–Mg–H$_2$O layer and the placements of the H$_2$O groups around the cations (Fig. 7*b,c,d*), the Na and Mg coordination polyhedra in this layer appear to be isolated, that is, not to be linked to one another. Note that the short Mg–OWa distance of 1.985 Å and the short Na–OWb distance of 1.721 Å do not correspond to bonds; these OW sites are vacant when the nearby cation sites are occupied.

The bond-valence sums (BVS) based on the As^{3+}–O parameters from Gagné and Hawthorne (2015), As^{3+}–Cl from Brese and O'Keeffe (1991) and NH$_4^+$–O from García-Rodríguez *et al.* (2000) are As1 = 2.98, As2 = 3.00, O = 2.08, N(NH$_4$) = 1.00 and Cl = 0.24 valence units (vu). The Cl BVS does not include hydrogen bond contributions from the partially occupied H$_2$O groups; however, very low BVS values are also observed for Cl in the lucabindiite (0.31 vu) and gajardoite (0.24 vu) structures, a phenomenon probably caused by the repulsive effect of the lone electron pair of the As^{3+}. The calculation of the BVS values for the components of the Na–Mg–H$_2$O layer is problematic because of the disorder and partial occupancies. Note that, while the Na and Mg site assignments are based upon bond lengths, the Mg–OWb distance (2.230 Å) suggests that some Na may occupy this site, as well.

References

Brese N.E. and O'Keeffe M. (1991) Bond-valence parameters for solids. *Acta Crystallographica*, **B47**, 192–197.

Cameron E.M., Leybourne M.I. and Palacios C. (2007) Atacamite in the oxide zone of copper deposits in northern Chile: involvement of deep formation waters? *Mineralium Deposita*, **42**, 205–218.

Chukanov N.V. (2014) *Infrared Spectra of Mineral Species: Extended library.* Springer-Verlag GmbH, Dordrecht–Heidelberg–New York–London, 1716 pp.

Chukanov N.V. and Chervonnyi A.D. (2016) *Infrared Spectroscopy of Minerals and Related Compounds.* Springer, Cham–Heidelberg–Dordrecht–New York–London, 1109 pp.

Gagné O.C. and Hawthorne F.C. (2015) Comprehensive derivation of bond-valence parameters for ion pairs involving oxygen. *Acta Crystallographica*, **B71**, 562–578.

Garavelli A., Mitolo D., Pinto D. and Vurro F. (2013) Lucabindiite, (K,NH$_4$)As$_4$O$_6$(Cl,Br), a new fumarole mineral from the "La Fossa" crater at Vulcano, Aeolian Islands, Italy. *American Mineralogist*, **98**, 470–477.

García-Rodríguez L., Rute-Pérez Á., Piñero J.R., and González-Silgo C. (2000) Bond-valence parameters for ammonium-anion interactions. *Acta Crystallographica*, **B56**, 565–569.

Gutiérrez H. (1975) *Informe sobre una rápida visita a la mina de arsénico nativo, Torrecillas.* Instituto de Investigaciones Geológicas, Iquique, Chile.

Kampf A.R., Sciberras M.J., Williams P.A., Dini M. and Molina Donoso A.A. (2013) Leverettite from the Torrecillas mine, Iquique Provence, Chile: the Co-analogue of herbertsmithite *Mineralogical Magazine*, **77**, 3047–3054.

Kampf A.R., Nash B.P., Dini M. and Molina Donoso A.A. (2016) Gajardoite, KCa$_{0.5}$As$^{3+}_4$O$_6$Cl$_2$·5H$_2$O, a new mineral related to lucabindiite and torrecillasite from the Torrecillas mine, Iquique Province, Chile. *Mineralogical Magazine*, **80**, 1265–1272.

Kampf A.R., Chukanov N.V., Möhn G., Dini M., Molina Donoso A.A. and Friis H. (2018a) Cuatrocapaite-(NH$_4$), IMA 2018-083. CNMNC Newsletter No. 46, December 2018, page 1371; *Mineralogical Magazine*, **82**, 1369–1379.

Kampf A.R., Chukanov N.V., Möhn G., Dini M., Molina Donoso A.A. and Friis H. (2018b) Cuatrocapaite-(K), IMA 2018-084. CNMNC Newsletter No. 46, December 2018, page 1372; *Mineralogical Magazine*, **82**, 1369–1379.

Kampf A.R., Nash B.P., Dini M. and Molina Donoso A.A. (2019) Camanchacaite, chinchorroite, espadaite, magnesiofluckite, picaite and ríosecoite: six new hydrogen-arsenate minerals from the Torrecillas mine, Iquique Province, Chile. *Mineralogical Magazine*, **83**, 655–671.

Mandarino J.A. (2007) The Gladstone–Dale compatibility of minerals and its use in selecting mineral species for further study. *The Canadian Mineralogist*, **45**, 1307–1324.

Mortimer C., Saric N. and Cáceres R. (1971) *Apuntes Sobre Algunas Minas de la Región Costera de la Provincia de Tarapacá.* Instituto de Investigaciones Geológicas, Santiago de Chile, Chile.

Oliveros V., Morata D., Aguirre L., Féraud G. and Fornari M. (2007) Jurassic to Early Cretaceous subduction-related magmatism in the Coastal Cordillera of northern Chile (18°30′–24° S): geochemistry and petrogenesis. *Revista Geológica de Chile*, **34**, 209–232.

Pimentel F. (1978) *Proyecto Arsenico Torrecillas.* Instituto de Investigaciones Geológicas, Iquique, Chile.

Rech J.A., Quade J. and Hart W.S. (2003) Isotopic evidence for the source of Ca and S in soil gypsum, anhydrite and calcite in the Atacama Desert, Chile. *Geochimica et Cosmochimica Acta*, **67**, 575–586.

Sheldrick G.M. (2015a) SHELXT – Integrated space-group and crystal-structure determination. *Acta Crystallographica*, **A71**, 3–8.

Sheldrick G.M. (2015b) Crystal Structure refinement with SHELX. *Acta Crystallographica*, **C71**, 3–8.

Wang F., Michalski G., Seo J. and Ge W. (2014) Geochemical, isotopic, and mineralogical constraints on atmospheric deposition in the hyper-arid Atacama Desert, Chile. *Geochimica et Cosmochimica Acta*, **135**, 29–48.